

Supplementary Information

Polytypism in Few-Layer Gallium Selenide

Soo Yeon Lim^a, Jae-Ung Lee^{a,b}, Jung Hwa Kim^{c,d}, Liangbo Liang^e, Xiangru Kong^e, Thi Thanh Huong Nguyen^f, Zonghoon Lee^{c,d}, Sunghae Cho^f and Hyeonsik Cheong^a

^a Department of Physics, Sogang University, Seoul 04107, Korea

^b Department of Physics, Ajou university, Suwon 16499, Korea

^c School of Materials Science and Engineering, Ulsan National Institute of Science and Technology (UNIST), Ulsan 44919, Korea

^d Center for Multidimensional Carbon Materials, Institute for Basic Science (IBS), Ulsan 44919, Korea

^e Center for Nanophase Materials Sciences, Oak Ridge National Laboratory, Oak Ridge, Tennessee 37831, United States

^f Department of Physics and Energy Harvest Storage Research Center, University of Ulsan, Ulsan 44610, Korea

E-mail: hcheong@sogang.ac.kr

Contents:

- **Fig. S1.** Optical and AFM images showing laser-induced degradation of few-layer GaSe
- **Fig. S2.** Ultra-low-frequency Raman spectra for 1-, 2-, 3-, 4-, 5-layer, and bulk GaSe in cross and parallel polarization configurations.
- **Fig. S3.** Polarization dependence of Raman peak intensities of (a) $A_1'(1)$, (b) E' , and (c) $A_1'(2)$ modes measured in the parallel polarization configuration, showing in-plane isotropy.
- **Fig. S4.** Raman spectra of 6- and 7-layer and bulk GaSe.
- **Note S1.** Raman tensor calculations for four polytypes of bulk GaSe in linear and circular polarization configurations.

- **Table S1.** Raman intensities of bulk GaSe in linear and circular polarization configurations.
- **Fig. S5.** Various trilayer GaSe samples measured in our work.
- **Fig. S6.** Circularly polarized Raman spectra from trilayer GaSe samples with four different types of the ultra-low-frequency Raman spectra.
- **Fig. S7.** Possible stacking sequences in trilayer GaSe.
- **Note S2.** Inter-layer bond polarizability model.
- **Table S2.** Simulated intensity ratios of the spots in the HR-S/TEM images for AA'B' and A'B'B stacking.
- **Fig. S8.** HR-TEM image and diffraction pattern from the area surrounding the Type 1 sample of Figure 5e.
- **References**

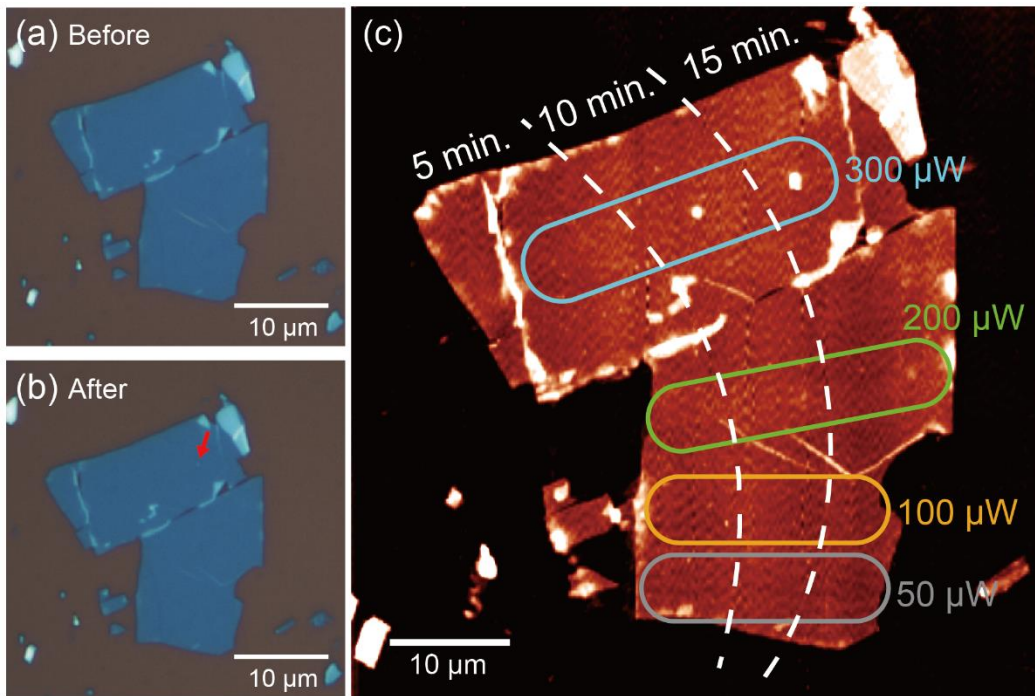


Fig. S1. Laser-induced degradation of few-layer GaSe by a 532-nm laser. Optical images taken (a) before and (b) after laser exposure in vacuum showing that damages are not visible except for the case of 15-min irradiation with the power of 300 μW . (c) AFM image of the sample after laser exposure. The laser powers and the exposure times are indicated. For 100 μW or below, no apparent change is observed. At 200 μW , a slight change is seen after 10 min. At 300 μW , obvious degradation is seen after 10 min.

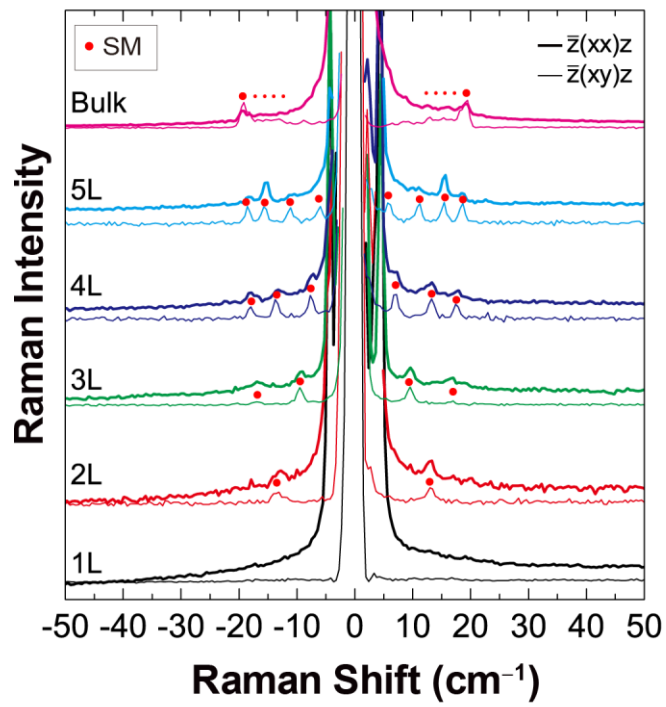


Fig. S2. Ultra-low-frequency Raman spectra for 1-, 2-, 3-, 4-, 5-layer, and bulk GaSe in cross and parallel polarization configurations.

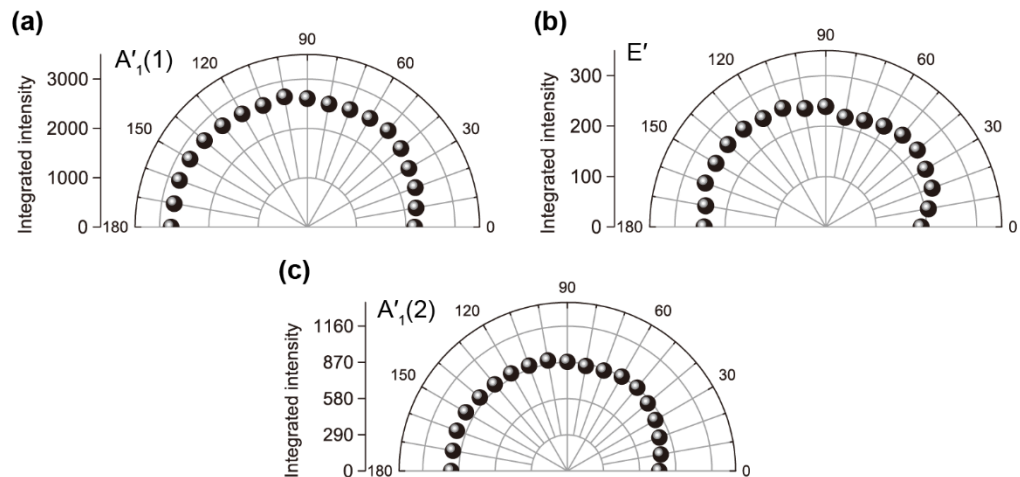


Fig. S3. Polarization dependence of Raman peak intensities of (a) $A'_1(2)$, (b) E' , and (c) $A'_1(2)$ modes measured in the parallel polarization configuration, showing in-plane isotropy.

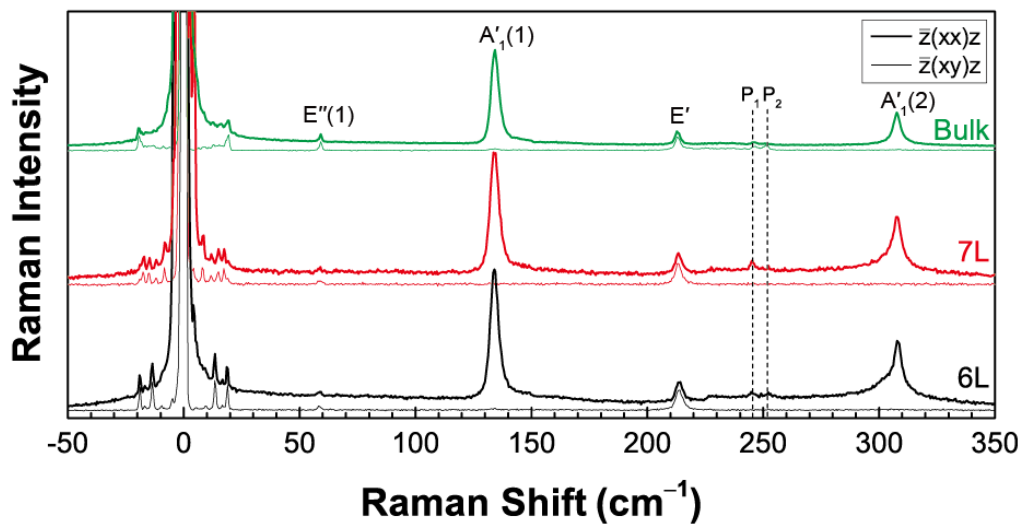


Fig. S4. Raman spectra of 6- and 7-layer and bulk GaSe. P_1 and P_2 are occasionally observed in thick samples.

Note S1. Raman tensor calculations for four polytypes of bulk GaSe in linear and circular polarization configurations^{S1, S2}

The β - and ε -GaSe have 24 normal vibrational modes with D_{6h}^4 and D_{3h}^1 space group, respectively. Since the γ -GaSe with C_{3v}^5 space group includes three layers in one unit cell, 36 normal modes exist. The δ -GaSe has C_{6v}^4 space group corresponding to 48 normal modes. The four different polytypes of bulk GaSe show the following irreducible representations at the zone center:

$$\begin{aligned}
 \Gamma_{\beta} &= 2A_{2u} + 2A_{1g} + 2B_{1u} + 2B_{2g} + 2E_{1u} + 2E_{2g} + 2E_{1g} + 2E_{2u} \\
 \Gamma_{\varepsilon} &= 4A_1' + 4A_2'' + 4E' + 4E'' \\
 \Gamma_{\gamma} &= 12A_1 + 12E \\
 \Gamma_{\delta} &= 8A_1 + 8B_1 + 8E_1 + 8E_2
 \end{aligned} \tag{S1}$$

The β -GaSe has 6 Raman active modes ($2A_{1g}$, $2E_{2g}$, and $2E_{1g}$ modes) and the ε -GaSe have 11 nondegenerate Raman active modes ($4A_1'$, $3E'$, and $4E_1''$). On the other hand, all the optical modes in γ -GaSe are both infrared and Raman active, so 22 nondegenerate Raman active modes exist. For the δ -GaSe, 7 A_1 and 7 E_1 modes except the acoustic modes are Raman allowed as well as 8 modes of E_2 .

The intensity of each mode is proportional to $|\hat{e}_s \cdot \vec{\mathbb{R}} \cdot \hat{e}_i|^2$, where \hat{e}_s and \hat{e}_i are polarizations of the scattered and incident photons, respectively, and $\vec{\mathbb{R}}$ is the Raman tensor. For the hexagonal (β -, ε -, and δ -) GaSe, the Raman tensors can be written as

$$\beta\text{-GaSe} : A_{1g} = \begin{pmatrix} a & 0 & 0 \\ 0 & a & 0 \\ 0 & 0 & b \end{pmatrix}, E_{1g} = \begin{pmatrix} 0 & 0 & 0 \\ 0 & 0 & c \\ 0 & c & 0 \end{pmatrix}, E_{1g} = \begin{pmatrix} 0 & 0 & -c \\ 0 & 0 & 0 \\ -c & 0 & 0 \end{pmatrix}, \quad (\text{S2})$$

$$E_{2g} = \begin{pmatrix} d & 0 & 0 \\ 0 & -d & 0 \\ 0 & 0 & 0 \end{pmatrix}, E_{2g} = \begin{pmatrix} 0 & -d & 0 \\ -d & 0 & 0 \\ 0 & 0 & 0 \end{pmatrix}$$

$$\varepsilon\text{-GaSe} : A'_1 = \begin{pmatrix} a & 0 & 0 \\ 0 & a & 0 \\ 0 & 0 & b \end{pmatrix}, E'' = \begin{pmatrix} 0 & 0 & 0 \\ 0 & 0 & c \\ 0 & c & 0 \end{pmatrix}, E'' = \begin{pmatrix} 0 & 0 & -c \\ 0 & 0 & 0 \\ -c & 0 & 0 \end{pmatrix}, \quad (\text{S3})$$

$$E'(x) = \begin{pmatrix} d & 0 & 0 \\ 0 & -d & 0 \\ 0 & 0 & 0 \end{pmatrix}, E'(y) = \begin{pmatrix} 0 & -d & 0 \\ -d & 0 & 0 \\ 0 & 0 & 0 \end{pmatrix}$$

$$\delta\text{-GaSe} : A_1(z) = \begin{pmatrix} a & 0 & 0 \\ 0 & a & 0 \\ 0 & 0 & b \end{pmatrix}, E_1(x) = \begin{pmatrix} 0 & 0 & c \\ 0 & 0 & 0 \\ c & 0 & 0 \end{pmatrix}, E_1(y) = \begin{pmatrix} 0 & 0 & 0 \\ 0 & 0 & c \\ 0 & c & 0 \end{pmatrix}, \quad (\text{S4})$$

$$E_2 = \begin{pmatrix} d & 0 & 0 \\ 0 & -d & 0 \\ 0 & 0 & 0 \end{pmatrix}, E_2 = \begin{pmatrix} 0 & -d & 0 \\ -d & 0 & 0 \\ 0 & 0 & 0 \end{pmatrix}$$

where a , b , c and d are constants. On the other hand, γ -GaSe has the Raman tensors:

$$\gamma\text{-GaSe} : A_1(z) = \begin{pmatrix} a & 0 & 0 \\ 0 & a & 0 \\ 0 & 0 & b \end{pmatrix}, E(x) = \begin{pmatrix} 0 & c & d \\ c & 0 & 0 \\ d & 0 & 0 \end{pmatrix}, E(y) = \begin{pmatrix} c & 0 & 0 \\ 0 & -c & d \\ 0 & d & 0 \end{pmatrix} \quad (\text{S5})$$

For the case of the linearly polarized light in back-scattering geometry, we can write down the incident and scattered light vectors as $\hat{e}_i = (\cos\theta_i \quad \sin\theta_i \quad 0)$ and $\hat{e}_s = (\cos\theta_s \quad \sin\theta_s \quad 0)$, respectively. The angles θ_i and θ_s are angle of the incident and scattered light polarization with respect to an arbitrary reference direction 0° . Therefore, the intensities depending on the polarization angle of A_{1g} modes for β -GaSe, for example, can be calculated as

$$I_{A_{1g}} \propto \left| \hat{e}_s \cdot \vec{R} \cdot \hat{e}_i \right|^2 = \left| \begin{pmatrix} \cos \theta_s & \sin \theta_s & 0 \end{pmatrix} \begin{pmatrix} a & 0 & 0 \\ 0 & a & 0 \\ 0 & 0 & b \end{pmatrix} \begin{pmatrix} \cos \theta_i \\ \sin \theta_i \\ 0 \end{pmatrix} \right|^2 = a^2 |\cos(\theta_i - \theta_s)|^2 \quad (S6)$$

If the incident and scattered light are perpendicular, the term is zero. Therefore, we can only observe the A_{1g} modes in the parallel polarization configuration and not in the cross polarization configuration. Since the A'_1 mode for ε -GaSe and $A_1(z)$ modes for δ -GaSe and γ -GaSe have the identical form of the Raman tensors, the polarization dependences are the same.

In contrast to the A modes, some E modes are forbidden in back-scattering geometry although they are Raman active. The Raman tensors of two E_{1g} modes for β -GaSe, two of E'' modes for ε -GaSe, and $E_1(x)$ and $E_1(y)$ modes for δ -GaSe have no elements in the first and second columns and rows. Therefore, these E modes are forbidden in the back-scattering geometry. On the other hand, the intensities of two E_{2g} modes for β -GaSe depending on the polarization angle are

$$I_{E_{2g}} \propto \left| \begin{pmatrix} \cos \theta_s & \sin \theta_s & 0 \end{pmatrix} \begin{pmatrix} d & 0 & 0 \\ 0 & -d & 0 \\ 0 & 0 & 0 \end{pmatrix} \begin{pmatrix} \cos \theta_i \\ \sin \theta_i \\ 0 \end{pmatrix} \right|^2 = d^2 |\cos(\theta_i + \theta_s)|^2, \quad (S7)$$

$$I_{E_{2g}} \propto \left| \begin{pmatrix} \cos \theta_s & \sin \theta_s & 0 \end{pmatrix} \begin{pmatrix} 0 & -d & 0 \\ -d & 0 & 0 \\ 0 & 0 & 0 \end{pmatrix} \begin{pmatrix} \cos \theta_i \\ \sin \theta_i \\ 0 \end{pmatrix} \right|^2 = d^2 |\sin(\theta_i + \theta_s)|^2 \quad (S8)$$

Since these two E_{2g} modes are degenerate, the polarization dependence has a superposed form of the two modes, resulting in the total intensity proportional to a constant d^2 . Therefore, the E_{2g} modes can be observed regardless of the polarization configuration. The $E'(x)$ and $E'(y)$ modes

for ε -GaSe and the E_2 modes for δ -GaSe have the identical tensor forms, leading to the identical polarization dependences.

The Raman tensors of the $E(x)$ and $E(y)$ modes for the γ -GaSe are $\begin{pmatrix} 0 & c & d \\ c & 0 & 0 \\ d & 0 & 0 \end{pmatrix}$ and $\begin{pmatrix} c & 0 & 0 \\ 0 & -c & d \\ 0 & d & 0 \end{pmatrix}$,

respectively. The intensities are

$$I_{E(x)} \propto \left| \begin{pmatrix} \cos \theta_s & \sin \theta_s & 0 \end{pmatrix} \begin{pmatrix} 0 & c & d \\ c & 0 & 0 \\ d & 0 & 0 \end{pmatrix} \begin{pmatrix} \cos \theta_i \\ \sin \theta_i \\ 0 \end{pmatrix} \right|^2 = c^2 |\sin(\theta_i + \theta_s)|^2 \text{ and} \quad (\text{S9})$$

$$I_{E(y)} \propto \left| \begin{pmatrix} \cos \theta_s & \sin \theta_s & 0 \end{pmatrix} \begin{pmatrix} c & 0 & 0 \\ 0 & -c & d \\ 0 & d & 0 \end{pmatrix} \begin{pmatrix} \cos \theta_i \\ \sin \theta_i \\ 0 \end{pmatrix} \right|^2 = c^2 |\cos(\theta_i + \theta_s)|^2, \quad (\text{S10})$$

the same as the case of the E_{2g} modes for β -GaSe: the E modes for γ -GaSe have no polarization dependence.

Consequently, for linearly polarization configuration, all the A modes are observed in the parallel polarization configuration and not in the cross polarization configuration. The E_{1g} mode for β -GaSe, E'' mode for ε -GaSe, and $E_1(x)$ and $E_1(y)$ modes for δ -GaSe are not allowed in back-scattering geometry. All the other E modes for all the polytypes are allowed and have no polarization dependence. The results are summarized in Table S1.

Circularly polarized light in back-scattering geometry is represented by $\sigma_{\pm} = \frac{1}{\sqrt{2}}(1 \mp i \ 0)$.

The intensities of A_{1g} modes for all the polytypes are proportional to a^2 when the incident and

scattered light have the same polarizations $[(\sigma + \sigma+)$ or $(\sigma - \sigma-)]$ whereas the intensity is zero with the opposite polarizations $[(\sigma + \sigma-)$ or $(\sigma - \sigma+)]$, according to the following calculations:

$$\begin{aligned}
|\sigma^\dagger(+)\cdot\vec{\mathbf{R}}\cdot\sigma(+)|_{A_{1g}}^2 &\propto \frac{1}{4} \left| (1 \ i \ 0) \begin{pmatrix} a & 0 & 0 \\ 0 & a & 0 \\ 0 & 0 & b \end{pmatrix} \begin{pmatrix} 1 \\ -i \\ 0 \end{pmatrix} \right|^2 = \frac{1}{4} |a+a+0|^2 = a^2 \\
|\sigma^\dagger(-)\cdot\vec{\mathbf{R}}\cdot\sigma(-)|_{A_{1g}}^2 &\propto \frac{1}{4} \left| (1 \ -i \ 0) \begin{pmatrix} a & 0 & 0 \\ 0 & a & 0 \\ 0 & 0 & b \end{pmatrix} \begin{pmatrix} 1 \\ i \\ 0 \end{pmatrix} \right|^2 = \frac{1}{4} |a+a+0|^2 = a^2 \\
|\sigma^\dagger(+)\cdot\vec{\mathbf{R}}\cdot\sigma(-)|_{A_{1g}}^2 &\propto \frac{1}{4} \left| (1 \ i \ 0) \begin{pmatrix} a & 0 & 0 \\ 0 & a & 0 \\ 0 & 0 & b \end{pmatrix} \begin{pmatrix} 1 \\ i \\ 0 \end{pmatrix} \right|^2 = \frac{1}{4} |a-a+0|^2 = 0 \\
|\sigma^\dagger(-)\cdot\vec{\mathbf{R}}\cdot\sigma(+)|_{A_{1g}}^2 &\propto \frac{1}{4} \left| (1 \ -i \ 0) \begin{pmatrix} a & 0 & 0 \\ 0 & a & 0 \\ 0 & 0 & b \end{pmatrix} \begin{pmatrix} 1 \\ -i \\ 0 \end{pmatrix} \right|^2 = \frac{1}{4} |a-a+0|^2 = 0
\end{aligned} \tag{S11}$$

All the other A modes for other polytypes have the same polarization dependences.

As we mentioned above, two E_{1g} modes for β -GaSe, two of the E'' modes for ε -GaSe, and the $E_1(x)$ and $E_1(y)$ modes for δ -GaSe are forbidden in back-scattering geometry. The Raman tensors of the E_{2g} modes for β -GaSe, the $E'(x)$ and $E'(y)$ modes for ε -GaSe, and the E_2 modes

for δ -GaSe are $\begin{pmatrix} d & 0 & 0 \\ 0 & -d & 0 \\ 0 & 0 & 0 \end{pmatrix}$ and $\begin{pmatrix} 0 & -d & 0 \\ -d & 0 & 0 \\ 0 & 0 & 0 \end{pmatrix}$. These show opposite tendency compared to the A

modes in terms of the polarization dependences.

$$\left| \sigma^\dagger(+)\cdot\vec{\mathbf{R}}\cdot\sigma(+)\right|_{E_{2g}, E'(x), E_2}^2 \propto \frac{1}{4} \left| \begin{pmatrix} 1 & i & 0 \end{pmatrix} \begin{pmatrix} d & 0 & 0 \\ 0 & -d & 0 \\ 0 & 0 & 0 \end{pmatrix} \begin{pmatrix} 1 \\ -i \\ 0 \end{pmatrix} \right|^2 = \frac{1}{4} |d-d+0|^2 = 0$$

$$\left| \sigma^\dagger(-)\cdot\vec{\mathbf{R}}\cdot\sigma(-)\right|_{E_{2g}, E'(x), E_2}^2 \propto \frac{1}{4} \left| \begin{pmatrix} 1 & -i & 0 \end{pmatrix} \begin{pmatrix} d & 0 & 0 \\ 0 & -d & 0 \\ 0 & 0 & 0 \end{pmatrix} \begin{pmatrix} 1 \\ i \\ 0 \end{pmatrix} \right|^2 = \frac{1}{4} |d-d+0|^2 = 0$$

$$\left| \sigma^\dagger(+)\cdot\vec{\mathbf{R}}\cdot\sigma(-)\right|_{E_{2g}, E'(x), E_2}^2 \propto \frac{1}{4} \left| \begin{pmatrix} 1 & i & 0 \end{pmatrix} \begin{pmatrix} d & 0 & 0 \\ 0 & -d & 0 \\ 0 & 0 & 0 \end{pmatrix} \begin{pmatrix} 1 \\ i \\ 0 \end{pmatrix} \right|^2 = \frac{1}{4} |d+d+0|^2 = d^2$$

$$\left| \sigma^\dagger(-)\cdot\vec{\mathbf{R}}\cdot\sigma(+)\right|_{E_{2g}, E'(x), E_2}^2 \propto \frac{1}{4} \left| \begin{pmatrix} 1 & -i & 0 \end{pmatrix} \begin{pmatrix} d & 0 & 0 \\ 0 & -d & 0 \\ 0 & 0 & 0 \end{pmatrix} \begin{pmatrix} 1 \\ -i \\ 0 \end{pmatrix} \right|^2 = \frac{1}{4} |d+d+0|^2 = d^2 \quad (\text{S12})$$

Similarly, for $\begin{pmatrix} 0 & -d & 0 \\ -d & 0 & 0 \\ 0 & 0 & 0 \end{pmatrix}$, the results are exactly same.

The Raman tensors of $E(x) = \begin{pmatrix} 0 & c & d \\ c & 0 & 0 \\ d & 0 & 0 \end{pmatrix}$, $E(y) = \begin{pmatrix} c & 0 & 0 \\ 0 & -c & d \\ 0 & d & 0 \end{pmatrix}$ for δ -GaSe result in the identical

dependence. For the $E(x)$ and $E(y)$ mode, the intensity is zero in the same polarization configuration and proportional to c^2 in the opposite polarization configuration.

$$\left| \sigma^\dagger(+)\cdot\vec{\mathbf{R}}\cdot\sigma(+)\right|_{E(x)}^2 \propto \frac{1}{4} \left| \begin{pmatrix} 1 & i & 0 \end{pmatrix} \begin{pmatrix} 0 & c & d \\ c & 0 & 0 \\ d & 0 & 0 \end{pmatrix} \begin{pmatrix} 1 \\ -i \\ 0 \end{pmatrix} \right|^2 = \frac{1}{4} |ic-ic+0|^2 = 0$$

$$|\sigma^\dagger(-) \cdot \vec{R} \cdot \sigma(-)|_{E(x)}^2 \propto \frac{1}{4} \left| (1 \quad -i \quad 0) \begin{pmatrix} 0 & c & d \\ c & 0 & 0 \\ d & 0 & 0 \end{pmatrix} \begin{pmatrix} 1 \\ i \\ 0 \end{pmatrix} \right|^2 = \frac{1}{4} |-ic + ic + 0|^2 = 0$$

$$|\sigma^\dagger(+) \cdot \vec{R} \cdot \sigma(-)|_{E(x)}^2 \propto \frac{1}{4} \left| (1 \quad i \quad 0) \begin{pmatrix} 0 & c & d \\ c & 0 & 0 \\ d & 0 & 0 \end{pmatrix} \begin{pmatrix} 1 \\ i \\ 0 \end{pmatrix} \right|^2 = \frac{1}{4} |2ic|^2 = c^2$$

$$|\sigma^\dagger(-) \cdot \vec{R} \cdot \sigma(+)|_{E(x)}^2 \propto \frac{1}{4} \left| (1 \quad -i \quad 0) \begin{pmatrix} 0 & c & d \\ c & 0 & 0 \\ d & 0 & 0 \end{pmatrix} \begin{pmatrix} 1 \\ -i \\ 0 \end{pmatrix} \right|^2 = \frac{1}{4} |-2ic|^2 = c^2 \quad (\text{S13})$$

Consequently, the A modes are observed in the same polarization configuration and the E modes in the opposite polarization configuration. It is possible to differentiate the A and E modes by using the circularly polarized light. The results are summarized in Table S1.

Table S1. Raman intensities of bulk GaSe in linear and circular polarization configurations

Polytype	Vibrational modes	$\bar{z}(xx)z$	$\bar{z}(xy)z$	$\sigma \pm \sigma \pm$	$\sigma \pm \sigma \mp$
β	$A_{1g} = \begin{pmatrix} a & 0 & 0 \\ 0 & a & 0 \\ 0 & 0 & b \end{pmatrix}$	$\propto a^2$	0	$\propto a^2$	0
	$E_{1g} = \begin{pmatrix} 0 & 0 & 0 \\ 0 & 0 & c \\ 0 & c & 0 \end{pmatrix}$	0	0	0	0
	$E_{1g} = \begin{pmatrix} 0 & 0 & -c \\ 0 & 0 & 0 \\ -c & 0 & 0 \end{pmatrix}$				
	$E_{2g} = \begin{pmatrix} d & 0 & 0 \\ 0 & -d & 0 \\ 0 & 0 & 0 \end{pmatrix}$	$\propto d^2$	$\propto d^2$	0	$\propto d^2$
	$E_{2g} = \begin{pmatrix} 0 & -d & 0 \\ -d & 0 & 0 \\ 0 & 0 & 0 \end{pmatrix}$				
ε	$A'_1 = \begin{pmatrix} a & 0 & 0 \\ 0 & a & 0 \\ 0 & 0 & b \end{pmatrix}$	$\propto a^2$	0	$\propto a^2$	0
	$E'' = \begin{pmatrix} 0 & 0 & 0 \\ 0 & 0 & c \\ 0 & c & 0 \end{pmatrix}$	0	0	0	0
	$E'' = \begin{pmatrix} 0 & 0 & -c \\ 0 & 0 & 0 \\ -c & 0 & 0 \end{pmatrix}$				
	$E'(x) = \begin{pmatrix} d & 0 & 0 \\ 0 & -d & 0 \\ 0 & 0 & 0 \end{pmatrix}$	$\propto d^2$	$\propto d^2$	0	$\propto d^2$
	$E'(y) = \begin{pmatrix} 0 & -d & 0 \\ -d & 0 & 0 \\ 0 & 0 & 0 \end{pmatrix}$				
δ	$A_1(z) = \begin{pmatrix} a & 0 & 0 \\ 0 & a & 0 \\ 0 & 0 & b \end{pmatrix}$	$\propto a^2$	0	$\propto a^2$	0
	$E_1(x) = \begin{pmatrix} 0 & 0 & c \\ 0 & 0 & 0 \\ c & 0 & 0 \end{pmatrix}$	0	0	0	0
	$E_1(y) = \begin{pmatrix} 0 & 0 & 0 \\ 0 & 0 & c \\ 0 & c & 0 \end{pmatrix}$				
	$E_2 = \begin{pmatrix} d & 0 & 0 \\ 0 & -d & 0 \\ 0 & 0 & 0 \end{pmatrix}$	$\propto d^2$	$\propto d^2$	0	$\propto d^2$
	$E_2 = \begin{pmatrix} 0 & -d & 0 \\ -d & 0 & 0 \\ 0 & 0 & 0 \end{pmatrix}$				
γ	$A_1(z) = \begin{pmatrix} a & 0 & 0 \\ 0 & a & 0 \\ 0 & 0 & b \end{pmatrix}$	$\propto a^2$	0	$\propto a^2$	0
	$E(x) = \begin{pmatrix} 0 & c & d \\ c & 0 & 0 \\ d & 0 & 0 \end{pmatrix}$	$\propto c^2$	$\propto c^2$	0	$\propto c^2$
	$E(y) = \begin{pmatrix} c & 0 & 0 \\ 0 & -c & d \\ 0 & d & 0 \end{pmatrix}$				

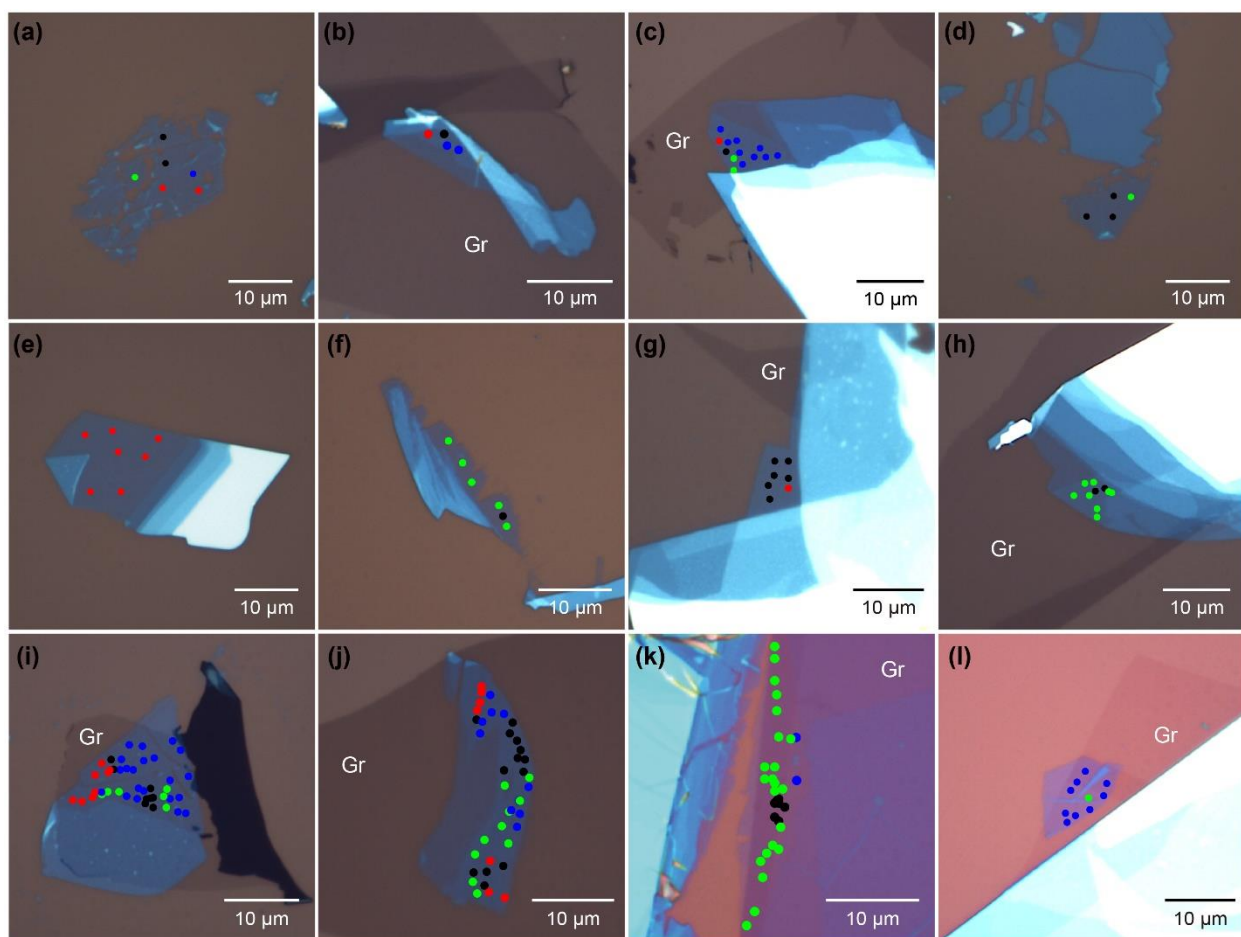


Fig. S5. Various trilayer GaSe samples measured in our work. The colored circles indicate the spots where Raman spectra were taken, with the color corresponding to the type of the ultra-low-frequency Raman spectrum: Type 1 (black), Type 2 (red), Type 3 (green), and Type 4 (blue).

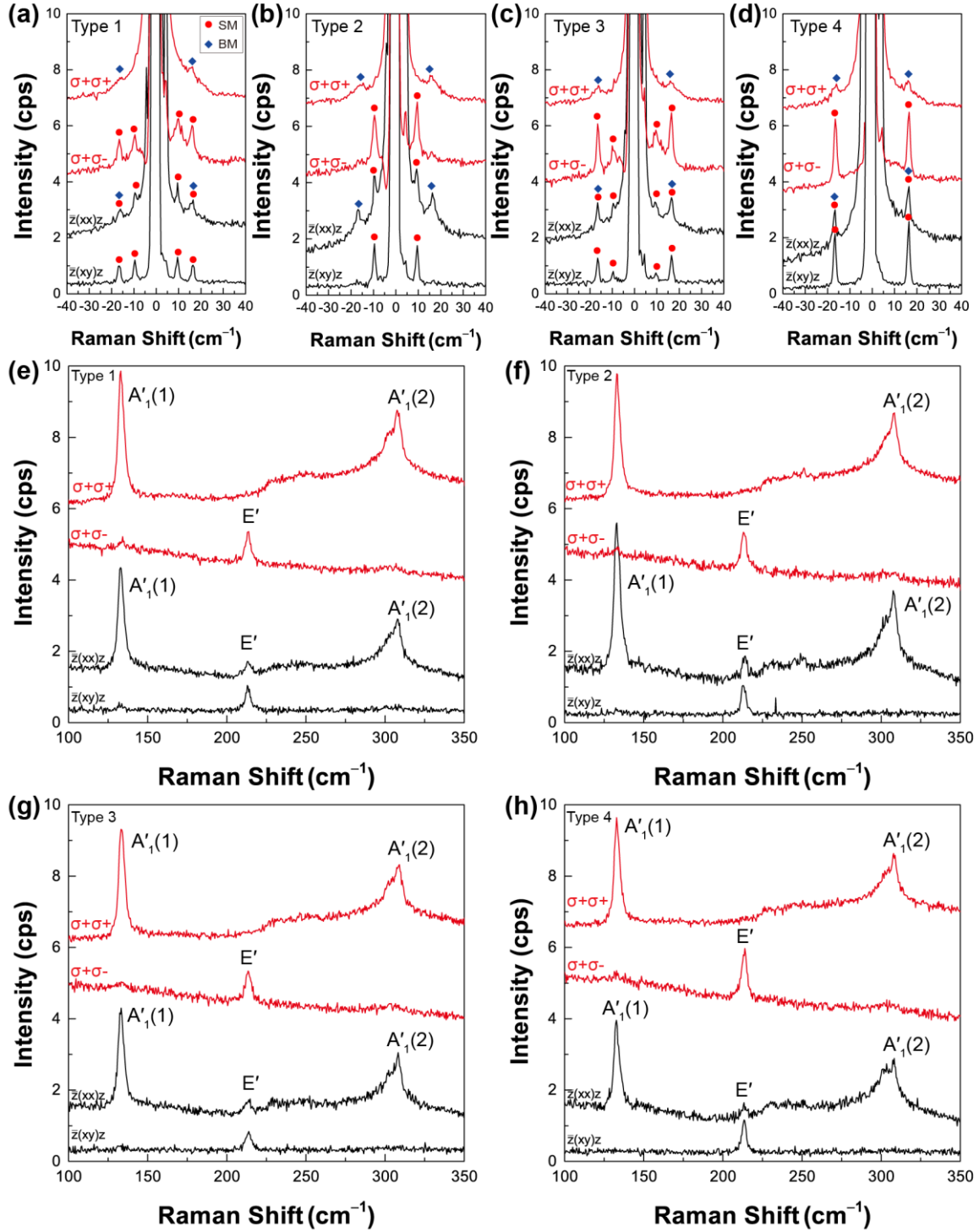


Fig. S6. Circularly polarized Raman spectra from trilayer GaSe samples with four different types of the ultra-low-frequency Raman spectra: (a), (e) Type 1, (b), (f) Type 2, (c), (g) Type 3, and (d), (h) Type 4.

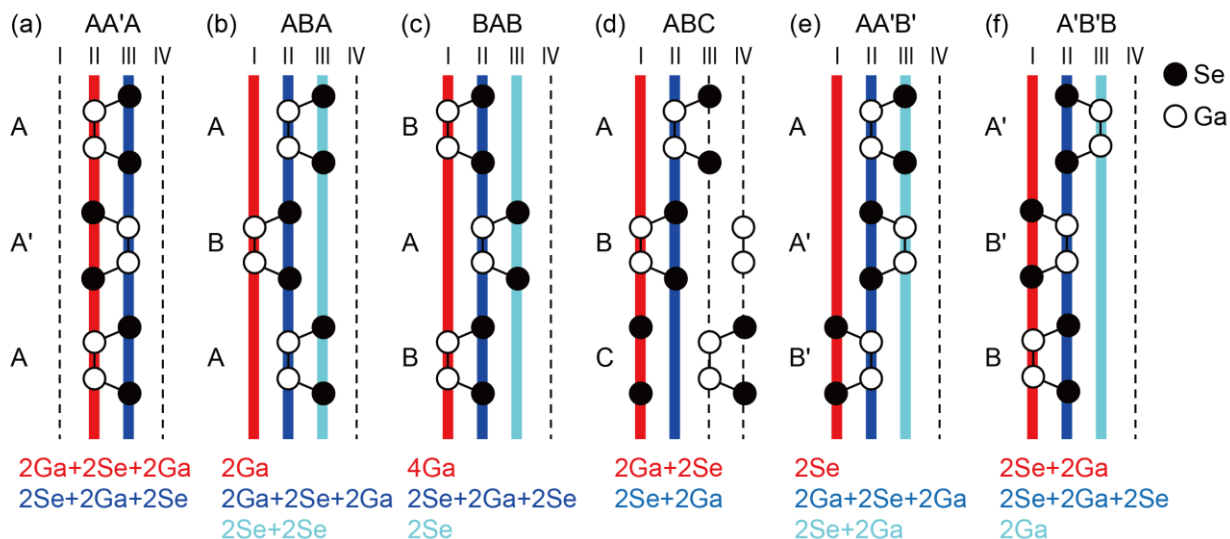


Fig. S7. Possible stacking sequences in trilayer GaSe. Each column consists of different atoms in the (a) AA'A, (b) ABA, (c) BAB, (e) AA'B', and (f) A'B'B, stacking sequences, whereas (d) all the columns in the ABC stacking sequences have the same atoms, two Ga and two Se, which is consistent with S/TEM results.

Note S2. Inter-layer bond polarizability model^{S3}

In addition to the first-principles DFT method, Raman intensities of low-frequency inter-layer modes in 2D materials can also be computed by a simple inter-layer bond polarizability model.^{S3} This model can provide more physical insights compared to the DFT approach. Generally speaking, Raman intensity of each normal mode is proportional to the change of the system's polarizability with respect to the normal coordinates of the corresponding vibration, and so obtaining the polarizability change by the vibration is crucial for calculating the intensity. For an inter-layer vibration mode, each layer oscillates as a quasi-rigid body, and therefore it can be treated as a single object. For the layer i , if the derivative of the system's polarizability with respect to its displacement is α'_i and its displacement during the inter-layer vibration is Δr_i , the change of the polarizability by this displacement is $\Delta\alpha_i = \alpha'_i \cdot \Delta r_i$. The total change of the system's polarizability by the inter-layer vibration is the sum of the changes of every layer: $\Delta\alpha = \sum_i \Delta\alpha_i = \sum_i \alpha'_i \cdot \Delta r_i$, where α'_i is related to the properties of the inter-layer bonds, including the inter-layer bond polarizabilities and the inter-layer bond vectors (lengths and directions).³ We note that if every layer moves in the same manner (i.e., $\Delta r_i = \Delta r$ for any layer i), the polarizability change of the system is given by $\Delta\alpha = (\sum_i \alpha'_i) \cdot \Delta r$. Such a motion corresponds to the translation of the whole system by Δr , and the translational invariance of the system's polarizability requires $\Delta\alpha = 0$, leading to a general relationship $\sum_i \alpha'_i = 0$. For a trilayer system, we then have $\alpha'_1 + \alpha'_2 + \alpha'_3 = 0$. The general form of α'_i can be simply determined based on the directions of the inter-layer bond vectors.^{S3,S4} Meanwhile, the displacement of each layer, Δr_i , can be determined by the linear chain model.^{S5} Finally, Raman intensity of the inter-layer vibration mode is obtained based on the

formula $I \propto \frac{n+1}{\omega} |\Delta\alpha|^2$, where $n = (e^{\frac{\hbar\omega}{k_B T}} - 1)^{-1}$ is the phonon occupation according to Bose–Einstein statistics and ω is the frequency of the vibration mode.

In trilayer GaSe, for an inter-layer shear vibration along the x direction, the polarizability change is $\Delta\alpha = \sum_i \alpha'_i \cdot \Delta x_i$, where α'_i can change notably with the stacking, since it is sensitive to the inter-layer bond polarizabilities and bond directions that vary with the stacking, according to the inter-layer bond polarizability model.^{S3, S4} Bilayer GaSe has two stacking patterns of AA' and AB, and the inter-layer bond properties are different as the relative layer-layer atomic alignments are different between AA' and AB stackings. For trilayer GaSe, there are a variety of stacking configurations, including AA'A, ABA, ABC, AA'B', and A'B'B. Note that both AA'B' and A'B'B originate from the bulk stacking AA'B'B. For AA'A stacking in trilayer GaSe, the top layer and bottom layer (i.e., layer 1 and layer 3) are in the equivalent positions, thereby giving $\alpha'_1 = \alpha'_3 = \beta'_1$ and subsequently $\alpha'_2 = -2\beta_1$ (recalling the aforementioned general relation $\alpha'_1 + \alpha'_2 + \alpha'_3 = 0$); for ABA stacking, the top layer and bottom layer are also in the equivalent positions, and it has the same form of inter-layer bond vectors as AA'A stacking but different inter-layer bond polarizabilities, therefore giving $\alpha'_1 = \alpha'_3 = \beta_2$ and subsequently $\alpha'_2 = -2\beta_2$ (note that β_1 and β_2 are related to the inter-layer bond polarizabilities of AA' and AB stackings, respectively); for ABC stacking, the layer-layer stacking assumes the same AB type as ABA stacking (i.e., BC stacking equivalent to BA), but layer 2 and layer 3 have different stacking directions and thus the opposite inter-layer bond directions compared to ABA stacking, thus yielding $\alpha'_1 = -\alpha'_3 = \beta_2$ and subsequently $\alpha'_2 = 0$; for AA'B' stacking, the situation is more complicated due to a mixture of AA' stacking between layer 1 and layer 2 and AB stacking between layer 2 and layer 3 (A'B' stacking equivalent to AB), and we can derive that

$(\alpha'_1, \alpha'_2, \alpha'_3) = (\beta_1, -\beta_1 + \beta_2, -\beta_2)$; for A'B'B stacking, it is a mixture of AB stacking between layer 1 and layer 2 and A'A stacking between layer 2 and layer 3 (B'B stacking equivalent to A'A, the reversed AA' stacking), and we can derive that $(\alpha'_1, \alpha'_2, \alpha'_3) = (\beta_2, -\beta_2 - \beta_1, \beta_1)$.

In summary, the polarizability derivatives of layer 1, layer 2 and layer 3 are $(\alpha'_1, \alpha'_2, \alpha'_3) = (\beta_1, -2\beta_1, \beta_1)$ for AA'A stacking; $(\beta_2, -2\beta_2, \beta_2)$ for ABA stacking; $(\beta_2, 0, -\beta_2)$ for ABC stacking; $(\beta_1, -\beta_1 + \beta_2, -\beta_2)$ for AA'B' stacking; $(\beta_2, -\beta_2 - \beta_1, \beta_1)$ for A'B'B stacking. On the other hand, for weakly coupled layered materials such as GaSe, graphene, MoS₂, etc, there are two inter-layer shear modes (S₁ and S₂) for the trilayer, and their frequencies and eigenvectors (i.e., layer displacements) show little dependence on the stacking pattern. Therefore, regardless of the stacking detail in trilayer GaSe, the normalized displacements of layer 1, layer 2 and layer 3 are

$(\Delta x_1, \Delta x_2, \Delta x_3) = \frac{1}{\sqrt{2}}(1, 0, -1)$ for the lower-frequency shear mode S₁, and $\frac{1}{\sqrt{1.5}}(0.5, -1, 0.5)$ for

the higher-frequency shear mode S₂, according to the linear chain model. Based on the formula

$\Delta\alpha = \sum_i \alpha'_i \cdot \Delta x_i$, we can subsequently obtain the polarizability changes by the shear vibrations as

follows:

$$\begin{aligned}
\Delta\alpha(\text{AA}'\text{A}, \text{S}_1) &= 0; & \Delta\alpha(\text{AA}'\text{A}, \text{S}_2) &= \sqrt{6}\beta_1; \\
\Delta\alpha(\text{ABA}, \text{S}_1) &= 0; & \Delta\alpha(\text{ABA}, \text{S}_2) &= \sqrt{6}\beta_2; \\
\Delta\alpha(\text{ABC}, \text{S}_1) &= \sqrt{2}\beta_2; & \Delta\alpha(\text{ABC}, \text{S}_2) &= 0; \\
\Delta\alpha(\text{AA}'\text{B}', \text{S}_1) &= \sqrt{0.5}(\beta_1 + \beta_2); & \Delta\alpha(\text{AA}'\text{B}', \text{S}_2) &= \sqrt{1.5}(\beta_1 - \beta_2); \\
\Delta\alpha(\text{A}'\text{B}'\text{B}, \text{S}_1) &= -\sqrt{0.5}(\beta_1 - \beta_2); & \Delta\alpha(\text{A}'\text{B}'\text{B}, \text{S}_2) &= \sqrt{1.5}(\beta_1 + \beta_2).
\end{aligned} \tag{S14}$$

Since $I \propto \frac{n+1}{\omega} |\Delta\alpha|^2$, Raman intensities of the shear modes S_1 and S_2 at different stacking

configurations in trilayer GaSe are the following:

$$\begin{aligned}
I(\text{AA}'\text{A}, S_1) &= 0; & I(\text{AA}'\text{A}, S_2) &\propto 6 \frac{n_2+1}{\omega_2} |\beta_1|^2; \\
I(\text{ABA}, S_1) &= 0; & I(\text{ABA}, S_2) &\propto 6 \frac{n_2+1}{\omega_2} |\beta_2|^2; \\
I(\text{ABC}, S_1) &\propto 2 \frac{n_1+1}{\omega_1} |\beta_2|^2; & I(\text{ABC}, S_2) &= 0; \\
I(\text{AA}'\text{B}', S_1) &\propto 0.5 \frac{n_1+1}{\omega_1} |\beta_1 + \beta_2|^2; & I(\text{AA}'\text{B}', S_2) &\propto 1.5 \frac{n_2+1}{\omega_2} |\beta_1 - \beta_2|^2; \\
I(\text{A}'\text{B}'\text{B}, S_1) &\propto 0.5 \frac{n_1+1}{\omega_1} |\beta_1 - \beta_2|^2; & I(\text{A}'\text{B}'\text{B}, S_2) &\propto 1.5 \frac{n_2+1}{\omega_2} |\beta_1 + \beta_2|^2,
\end{aligned} \tag{S15}$$

where n_1 and ω_1 are the occupation number and frequency of the shear mode S_1 , respectively; n_2 and ω_2 are the occupation number and frequency of the shear mode S_2 , respectively. According to the experimental data, $\omega_1 \approx 9.6 \text{ cm}^{-1}$ and $\omega_2 \approx 16.6 \text{ cm}^{-1}$, leading to $\frac{n_1+1}{\omega_1} = 2.30$ and $\frac{n_2+1}{\omega_2} = 0.78$

at room temperature. Therefore,

$$\begin{aligned}
I(\text{AA}'\text{A}, S_1) &= 0; & I(\text{AA}'\text{A}, S_2) &\propto 4.68 |\beta_1|^2; \\
I(\text{ABA}, S_1) &= 0; & I(\text{ABA}, S_2) &\propto 4.68 |\beta_2|^2; \\
I(\text{ABC}, S_1) &\propto 4.60 |\beta_2|^2; & I(\text{ABC}, S_2) &= 0;
\end{aligned} \tag{S16}$$

$$I(\text{AA}'\text{B}', S_1) \propto 1.15|\beta_1 + \beta_2|^2; \quad I(\text{AA}'\text{B}', S_2) \propto 1.17|\beta_1 - \beta_2|^2;$$

$$I(\text{A}'\text{B}'\text{B}, S_1) \propto 1.15|\beta_1 - \beta_2|^2; \quad I(\text{A}'\text{B}'\text{B}, S_2) \propto 1.17|\beta_1 + \beta_2|^2.$$

Table S2. Simulated intensity ratios of the spots in the HR-S/TEM images for AA'B' and A'B'B stacking.

Stacking sequences	Number of Ga atoms	Number of Se atoms	Intensity ratio
AA'B'	0	2	1
	2	2	1.51
	4	2	1.98
A'B'B	2	0	1
	2	2	1.65
	2	4	2.18

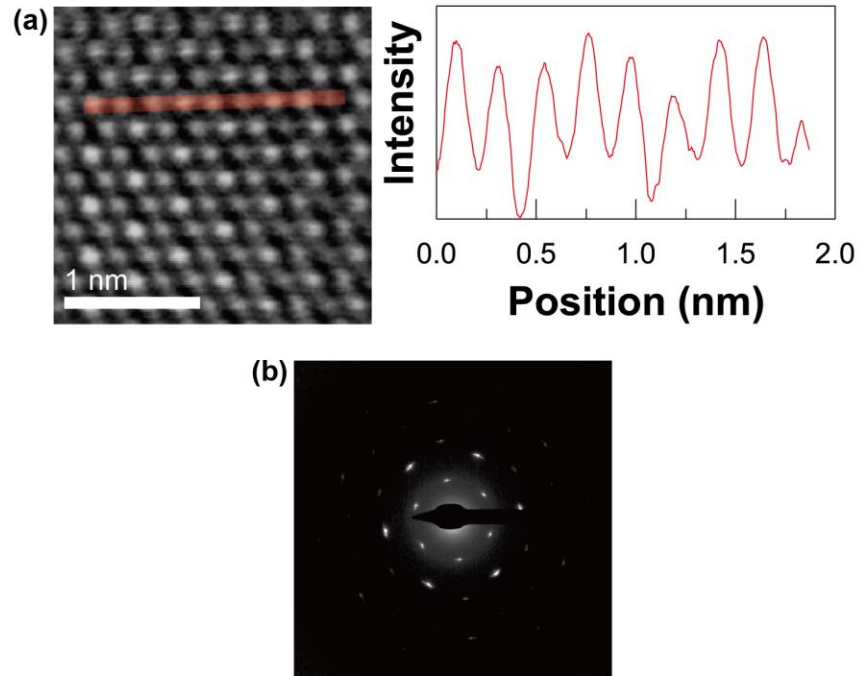


Fig. S8. (a) High-resolution TEM results from the surrounding region of the Type1 sample of Figure 5e showing an irregular intensity profile due to vacancies and (b) blurred diffraction pattern from the region showing poor crystallinity.

References

- S1 R. M. Hoff, J. C. Irwin and R. M. A. Lieth, *Can. J. Phys.*, 1975, **53**, 1606–1614.
- S2 A. Polian, K. Kunc and A. Kuhn, *Solid State Commun.*, 1976, **19**, 1079–1082.
- S3 L. Liang, A. A. Puretzky, B. G. Sumpter and V. Meunier, *Nanoscale*, 2017, **9**, 15340–15355.
- S4 L. Liang, J. Zhang, B. G. Sumpter, Q. H. Tan, P. H. Tan and V. Meunier, *ACS Nano*, 2017, **11**, 11777–11802.
- S5 P. H. Tan, W. P. Han, W. J. Zhao, Z. H. Wu, K. Chang, H. Wang, Y. F. Wang, N. Bonini, N. Marzari, N. Pugno, G. Savini, A. Lombardo and A. C. Ferrari, *Nat. Mater.*, 2012, **11**, 294–300.